PRAMANA
—journal of
physics

Vol. 51, Nos 1 & 2,
July/August 1998
pp. 205–216

Low x physics and structure functions

RAHUL BASU
The Institute of Mathematical Sciences, Chennai 600 113, India

Abstract. In this talk I review the behaviour of structure functions at low values of Bjorken x and discuss the theoretical underpinnings with particular attention to resummation schemes. I present the need for 'less inclusive' events to distinguish between various resummation schemes and discuss the various difficulties in differentiating experimentally between different schemes.

Keywords. QCD; deep inelastic scattering; proton structure.

PACS Nos 12.38; 12.85

1. Introduction

The wealth of data on structure functions at low x that has emerged from HERA in the last six years or so have provided fresh and interesting challenges to theorists to explain the steep rise in the structure function $F_2(x)$ along with many other new aspects of perturbative QCD at these hitherto unprobed kinematic regions. In this talk I will concentrate on structure functions and discuss in some detail the experimental data along with the theoretical attempts made to explain them. I will not be touching upon many of the other interesting aspects of low x QCD viz large rapidity gap events, quarkonia production, spin physics, photon structure functions and so on, most of which will be addressed by other speakers in this workshop.

The basic interaction picture is the usual DIS

$$e(k) + p(p) \rightarrow e(k') + X.$$

The following kinematic variables completely describe the process:

$$s = (k+p)^2 \simeq 4E_eE_p, \tag{1}$$

$$Q^2 = -q^2 \simeq 2E_eE_{e'}(1-\cos\theta), \tag{2}$$

$$y = \frac{p\cdot q}{p\cdot k} \simeq 1 - \frac{E_{e'}}{2E_e}(1-\cos\theta), \tag{3}$$

$$x = \frac{Q^2}{2p\cdot q} \simeq \frac{Q^2}{ys}, \tag{4}$$

$$W = (q+p)^2 \simeq -Q^2 + ys. \tag{5}$$

At HERA, a 27 GeV electron beam collides head-on with an 820 GeV proton beam giving

$$s \simeq 4E_eE_p \sim 10^5\ \text{GeV}^2$$

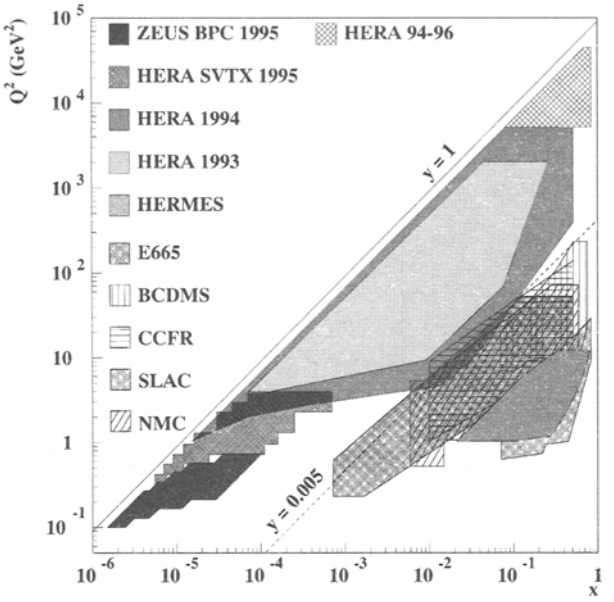

Figure 1. Phase space coverage of the F_2 measurements.

which is much larger than hitherto obtained at fixed target experiments. (Since 1994, the electron beam has been replaced by a positron beam at the same energy). As a result the two experiments H1 and ZEUS can measure the structure function F_2 in a completely new (x, Q^2) domain (see figure 1).

The Born cross section for single photon exchange in DIS is given by

$$\frac{\mathrm{d}^2\sigma}{\mathrm{d}x\mathrm{d}Q^2} = \frac{2\pi\alpha^2}{Q^2 x}\left[2(1-y) + \frac{y^2}{1+R}\right]F_2(x, Q^2), \tag{6}$$

where R is the photoproduction cross section ratio for longitudinal and transverse polarised photon, $R = \sigma_L/\sigma_T$. R has not been measured at HERA; therefore a QCD prescription based on parametrization of parton densities is used. Q^2 is directly measured from the scattered electron but x is calculated from Q^2 and y and therefore depends on the experimental resolution of y.

2. Measurement of $F_2(x, Q^2)$

The data for F_2 from H1 and ZEUS [1, 2] is shown in figures 2 and 3 along with some of the older fixed target data. It is clear that at fixed Q^2, F_2 rises with decreasing x down to the smallest Q^2, the steepness of the rise decreasing with decreasing Q^2. Similarly at fixed $x < 0.1$ F_2 rises with Q^2, the rise becoming steeper as x decreases. In fact, as seen in figure 2, up to $Q^2 \sim 0.85\,\mathrm{GeV}^2$ the data favour a parametrisation based on a soft pomeron such as that suggested by Donnachie and Landshoff [3]. For larger values of Q^2 ($Q^2 > 1.0\,\mathrm{GeV}^2$) the usual QCD based parametrisations of GRV or MRS [4, 5] give a good description of the data, as seen in figure 3.

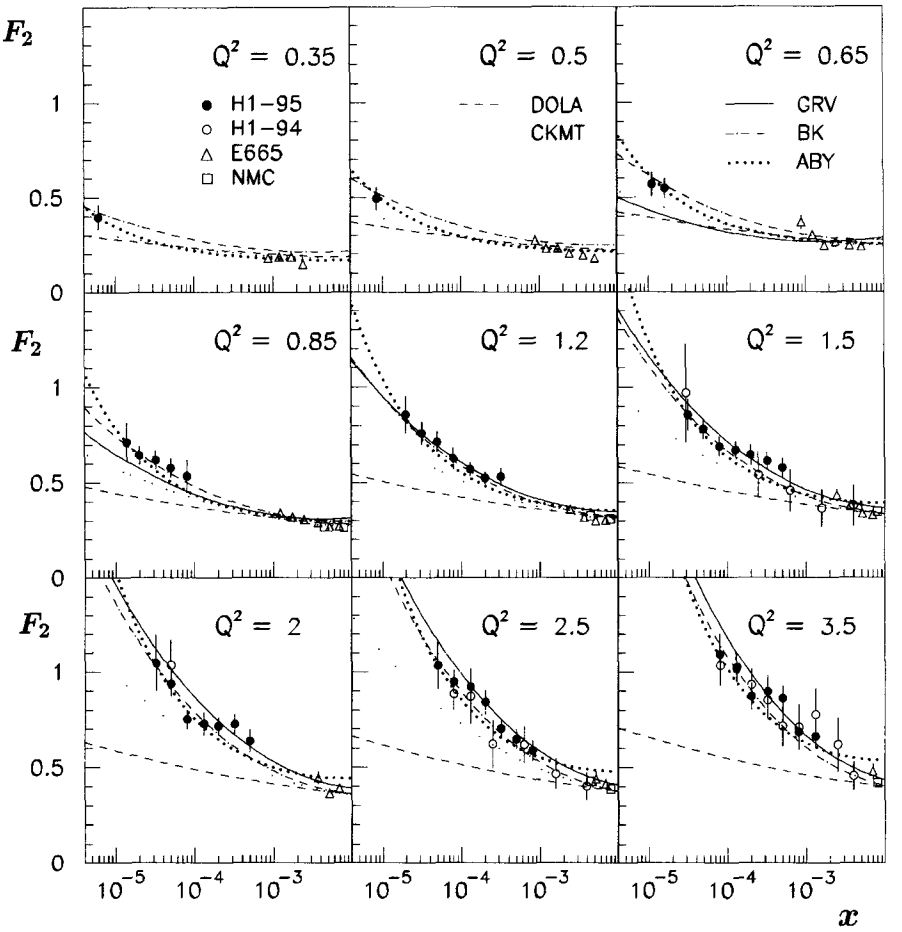

Figure 2. $F_2(x, Q^2)$ as a function of x for low Q^2. The Donnachie Landshoff (DOLA) and the standard QCD evolution represented by GRV are shown.

Thus the growth of the structure function for decreasing x, over three decades in Q^2 and over four decades in x is a clearly established fact and agrees remarkably well with a NLO QCD fit performed by H1. With the new data from HERA the gap between fixed target and the HERA experiments has been filled.

The H1 experiment has parametrised the rise of F_2 with x by $F \sim x^{-\lambda}$ at fixed Q^2 values. The result for λ as a function of Q^2 is shown in figure 4. It is clear from the figure that λ increases with increasing Q^2 reaching a value of around 0.4–0.5 around $Q^2 \sim 10^2$–$10^3\,\mathrm{GeV}^2$.

3. The behaviour of $F_2(x)$

The general behaviour of $F_2(x)$ can be understood as follows. Below $Q^2 \simeq 0.85\,\mathrm{GeV}^2$ the Regge theory predictions for a soft pomeron like behaviour seems to work quite well [3].

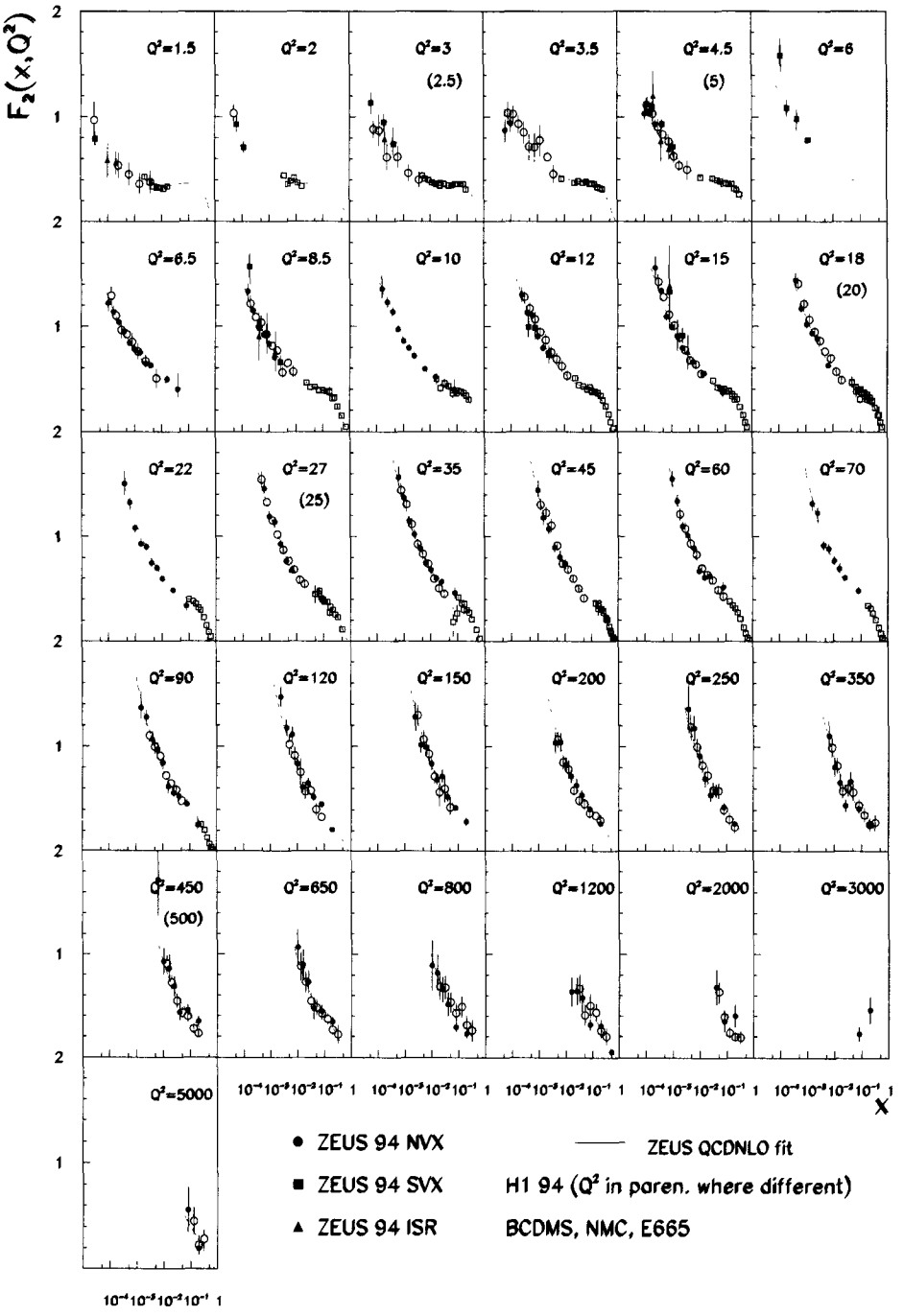

Figure 3. $F_2(x, Q^2)$ as a function of x for higher Q^2 compared with model predictions.

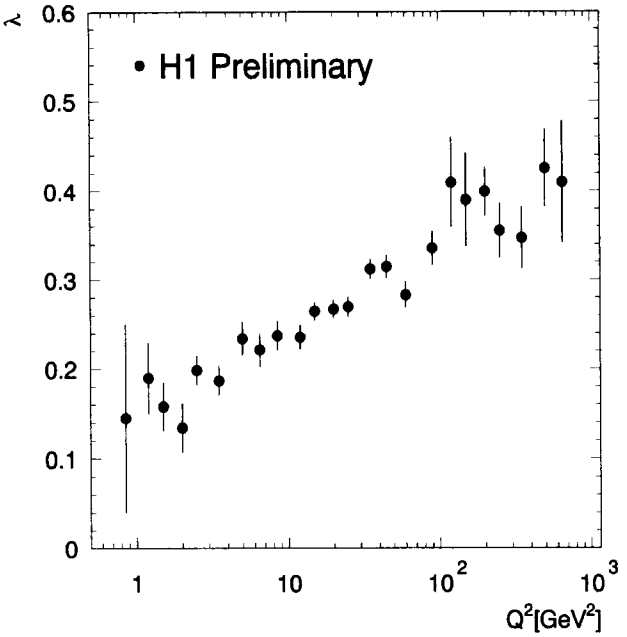

Figure 4. Variation of the exponent λ from fits of the form $F_2 \sim x^{-\lambda}$ at fixed Q^2 values and $x < 0.1$.

In this approach, the total cross section (for $\bar{p}p$, $K^{\pm}p$, $\pi^{\pm}p$ etc.) are fitted to a form

$$\sigma_{\text{tot}} = As^{\epsilon} + Bs^{-\eta}, \tag{7}$$

where $\epsilon = 0.08$ corresponds to a soft pomeron intercept $\alpha_{\mathbb{P}}(0) = 1 + \epsilon$ and $\eta = 0.45$ corresponds to the ρ meson trajectory intercept $\alpha = 1 + \eta$. Assuming a dipole model for the proton, the x dependence of F_2 can be extracted;

$$F_2^{\text{DOLA}}(x, Q^2) = Ax^{-0.08}\frac{Q^2}{Q^2 + a^2} + Bx^{0.45}\frac{Q^2}{Q^2 + b^2}. \tag{8}$$

Thus the DOLA analysis predicts a gentle rise of $x^{-0.08}$ for F_2 with decreasing x.

However this prediction, as we have seen from the data fails for $Q^2 > 0.85\,\text{GeV}^2$ where standard QCD evolution takes over, given generically by the GRV fits. For the rest of the section we shall be discussing the nature of this 'good' agreement of the data with QCD evolution.

The rise of F_2 as a function of x is explained by the usual DGLAP [7] evolution and also by more non-conventional dynamics like the BFKL evolution [8]. All these are QCD based evolution equations and hence it is appropriate to review the various approaches.

While perturbative QCD does not provide any information on hadronic structure. the idea of factorisation can be used to predict the change with scale of the probablility of finding parton i in the proton $f_{i/p}$. These are given by the various evolution equations, the differences between them being the approximations that are used to restrict the phase space for radiation. These approximations are then valid in regions of x, Q^2 where the

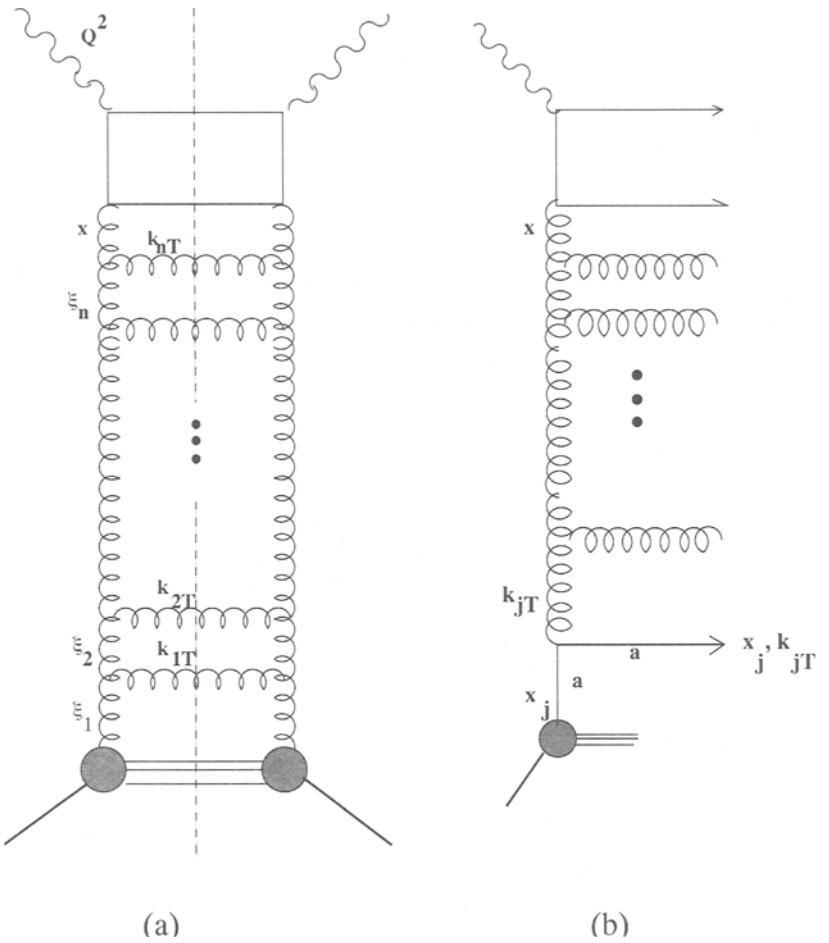

Figure 5. A gluon ladder diagram that contributes to the DLL or BFKL ladder summations (a) and a forward jet diagram (b).

selected contributions are the dominant ones. These therefore give different evolution equations (D) GLAP, DLL, BFKL ... (see also [10,11]).

To understand the leading log summation technique in the DGLAP approach, we use the Dokshitzer method [6]. At low values of x, the gluon is the dominant parton in the proton. He showed that the GLAP summation of the $(\alpha_s \log Q^2)^n$ terms amounts to a sum of gluon ladder diagrams of the type shown in figure 5(a) with n gluon rungs. The form of the gluon splitting function $P_{gg} \sim 6/x$ for small x gives the evolution of the gluon distribution function as

$$xg(x,Q^2) = \sum_n \left(\frac{3\alpha_s}{\pi}\right)^n \int^{Q^2} \frac{dk_{nT}^2}{k_{nT}^2} \cdots \int^{k_{3T}^2} \frac{dk_{2T}^2}{k_{2T}^2} \int^{k_{2T}^2} \frac{dk_{1T}^2}{k_{1T}^2} \times \int_x^1 \frac{d\xi_n}{\xi_n} \cdots \int_{\xi_3}^1 \frac{\xi_2}{\xi_2} \int_{\xi_2}^1 \frac{\xi_1}{\xi_1} \xi_1 g(\xi_1, Q_0^2). \quad (9)$$

It is clear that the $(\log Q^2)^n$ builds up from the nested k integrations. In fact this contribution comes from a region where the transverse momentum of the emitted gluons are strongly ordered

$$Q^2 \gg k_{nT}^2 \gg \cdots \gg k_{2T}^2 \gg k_{1T}^2. \tag{10}$$

This kinematic region is therefore relevant when Q^2 is large but x is not so small that $\alpha_s(Q^2)\ln(1/x)$ is large i.e

$$\alpha_s(Q^2)\ln(1/x) \ll \alpha_s(Q^2)\ln(Q^2/Q_0^2) < 1.$$

Similarly, the $(\log(1/x))^n$ term comes from the region where the longitudinal momentum fractions are strongly ordered

$$x \ll \xi_n \ll \cdots \ll \xi_2 \ll \xi_1. \tag{11}$$

In the region of small x the $\log(1/x)$ terms have also to be summed. With the assumption of $\xi_1 g(\xi_1, Q_0^2)$ approaching a constant, say G_0 the result we get is

$$\begin{aligned} xg(x,Q^2) &\sim \sum_n \left(\frac{3\alpha_s}{\pi}\right)^n \left\{\frac{1}{n!}\left[\ln\left(\frac{Q^2}{Q_0^2}\right)\right]^n\right\}\left\{\frac{1}{n!}\left[\ln\left(\frac{1}{x}\right)\right]^n G_0\right\} \\ &\sim G_0 \exp\left\{2\left[\frac{3\alpha_s}{\pi}\ln\left(\frac{Q^2}{Q_0^2}\right)\ln\left(\frac{1}{x}\right)\right]^{1/2}\right\} \end{aligned} \tag{12}$$

in the limit of large Q^2 and small x.

This is an example of an all order double leading log (DLL) summation of $\alpha_s \log Q^2 \log(1/x)$ obtained by summing the strongly ordered gluon ladder diagrams as we have just explained. It tells us that as x decreases, $xg(x,Q^2)$ increases faster than any power of $\log(1/x)$ but slower than any power of $1/x$. It is valid in a region where

$$\left\{\begin{matrix}\alpha_s(Q^2)\ln(Q^2/Q_0^2) \\ \alpha_s(Q^2)\ln(1/x)\end{matrix}\right\} \ll \alpha_s(Q^2)\ln(Q^2/Q_0^2)\ln(1/x) < 1.$$

If $k_{iT} \approx k_{i+1T}$ then we lose one power of $\log Q^2$. However, at small x, this can be compensated by a large $\log(1/x)$ factor. Relaxing the strong ordering constraint on the k_T's and summing just the $\log(1/x)$ in the small x region will give us the leading log summation in $\log(1/x)$ instead of DLL and we get

$$\begin{aligned} xg(x,Q^2) &\approx \sum_n \left(\frac{3\alpha_s}{\pi}\right)^n \frac{1}{n!}\left[c\ \log\left(\frac{1}{x}\right)\right]^n \\ &\sim \exp\left[\lambda \log\left(\frac{1}{x}\right)\right] \\ &\sim x^{-\lambda}, \end{aligned} \tag{13}$$

where $\lambda = (3\alpha_s/\pi)c$. This difficult summation was done rigorously by Balitskij, Fadin, Kuraev and Lipatov (BFKL) [8]. The constant $c = 4\ \log 2$ and so, for $\alpha_s \approx 0.2$, $\lambda \approx 0.5$. We have highly simplified the discussion of the BFKL equation, and in practise one needs to work in terms of the unintegrated gluon distribution $f(x,k_T^2)$ and integrate $f(x,k_T^2)/k_T^2$

to get the final gluon distribution. The BFKL region is therefore one where x is small and Q^2 is not large enough to reach the DLL regime.

We thus have two different predictions for the rise of F_2, the DLL (from the DGLAP evolution equations) and the BFKL. In principle it should therefore be possible to distinguish between these predictions by looking at the F_2 data from HERA. Unfortunately this is not that simple. The steepness of the rise of F_2 with decreasing x can be controlled by varying Q_0^2, or the starting distribution $g(\xi_1, Q_0^2)$. In addition, the set of equations based only on F_2 measurements is underconstrained and one needs one other measurement like the longitudinal structure function F_L in order to constrain the system fully.

The net consequence of the above is that the present data on F_2 does not distinguish between the BFKL and DGLAP (or for that matter the CCFM which embodies both) predictions.

One of the reasons that the data on F_2 is not sufficient is due to a phenomenon called k_T diffusion. Let us explain this in some detail. The BFKL equation predicts the behaviour of the unintegrated gluon distribution $f(x, k_T^2)$ to be

$$\frac{f(x,k_T^2)}{\sqrt{k_T^2}} \propto \frac{(x/x_0)^{-\lambda}}{\sqrt{2\pi\lambda'' \ln(x_0/x)}} \exp\left[-\frac{\ln^2(k_T^2/\bar{k_T^2})}{2\lambda'' \ln(x_0/x)}\right] \tag{14}$$

for fixed α_s. Here $\lambda = (3\alpha_s/\pi)4\ln 2 \simeq 0.5$ for $\alpha_s = 0.19$, $\lambda'' = (3\alpha_s/\pi)28\zeta(3)$. Thus the unintegrated gluon distribution exhibits a Gaussian in $\ln k_T^2$ with a width which increases with the BFKL evolution length $\sqrt{\ln(x_0/x)}$. This form implies that individual evolution paths follow a kind of random walk in k_T^2 and an ensemble of paths exhibits a diffusion pattern according to a Gaussian in $\ln k_T^2$. The net consequence of this is that k_T^2 can diffuse into a region of very small values where perturbation theory no longer holds. Contrast this with k_T ordering in DGLAP which ensures that the k_T's along a ladder are always constrained to remain within a region sufficiently removed from the infrared. The calculation of F_2 involving an integration over all k_T^2 in the BFKL formalism could therefore include diffusion of k_T into the IR region where perturbation theory fails. A possible solution is to study special final state configurations where diffusion into the IR region is minimised by fixing the start and end point of evolution for the above region.

This is the idea behind a suggestion by Mueller [9] on measuring an observable that is less inclusive than the F_2 measurement (in which none of the properties of the hadronic final state is measured). He suggests studying DIS events at small x containing an identified high-energy jet emitted close to the jet of proton fragments (see figure 5(b)). The identified jet originates from the parton labelled a. If we study events with x_j large (≥ 0.05) and x very small ($\approx 10^{-4}$) the ratio x/x_j will be sufficiently small to reveal the $(x/x_j)^{-\lambda}$ behaviour of the BKFL ladder. Details may be found in the references mentioned above. This study is currently under way and preliminary results are reported in [14]. We will have more to say on this later.

There are numerous other evolution equations and details of the current phenomenology of these evolution equations can be found in [13]. One of the by-products of the measurement of the structure function F_2 and its $\log Q^2$ evolution is that the gluon distribution inside the proton has been measured with greater accuracy (cf. figure 14 in [12]).

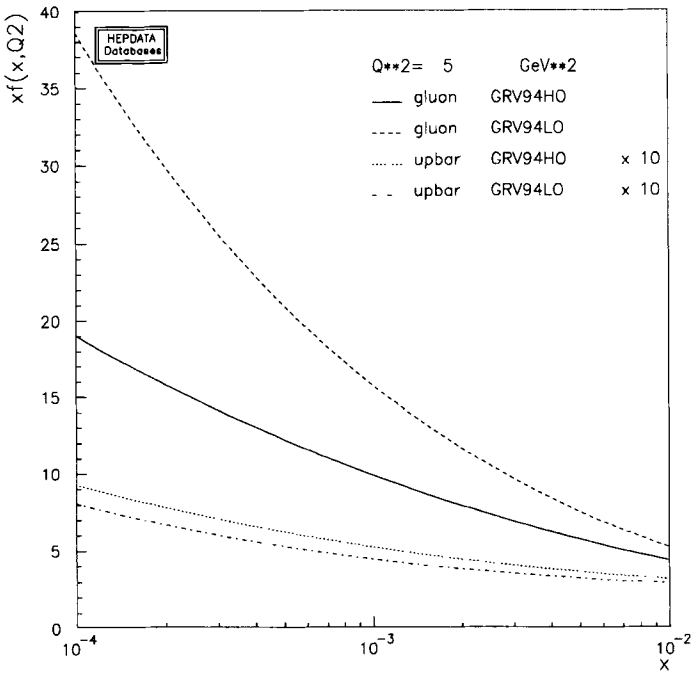

Figure 6. Input gluon and u quark densites at LO and NLO for GRV parametrization.

4. Forward jet events

Before we discuss issues of more exclusive events in order to differentiate between various evolution equations like DGLAP and BFKL, some discussion on the details of the phenomenology of these equations are in order. We have seen earlier the NLO-DGLAP indeed seems to work very well in describing the data down to $2\,\text{GeV}^2$. Do we therefore even need any other evolution equations like BFKL to describe the data on F_2. The answer is yes, because the 'perfect' fit of DGLAP to the data depends crucially on the input parton densities at low Q^2. To understand this fact, we need to compare the LO and NLO parton input densities. The fact that the GRV parametrization works so well is crucially dependent on the fact that the gluon densities have to be varied a lot. This is clear from figure 6 where the input gluon densities for LO and NLO are shown in the GRV parametrization. The evolution of F_2 is given by

$$\frac{\mathrm{d}F_2}{\mathrm{d}\ln Q^2} \sim P_{qg} \otimes g, \tag{15}$$

where

$$P_{qg} = \alpha_s P_{qg}^{(0)} \left[1 + 2.2\frac{3\alpha_s}{\pi}\frac{1}{x} + \cdots\right]. \tag{16}$$

Notice that the LO term is flat while the NLO term is steep in x. Thus a stable evolution of F_2 requires that the NLO steepness of P_{qg} has to be compensated by a gluon density

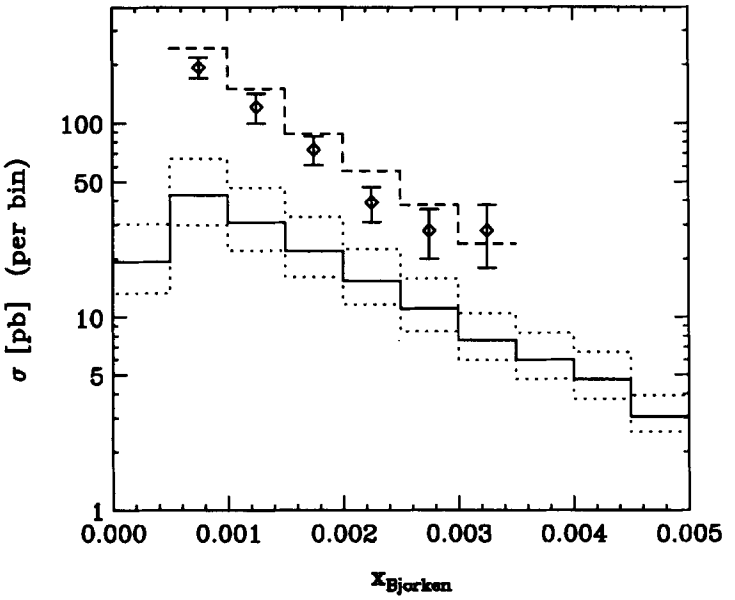

Figure 7. Forward jet cross section at HERA as a function of x. The solid histogram is the NLO MEPJET (DGLAP) result for the scale choice $\mu_R^2 = \mu_F^2 = \xi(0.5\sum k_T)^2$ with $\xi = 1$. The two dotted histograms show the uncertainty of the NLO prediction, corresponding to a variation of ξ between 0.1 and 10. The BFKL result of Bartels *et al* [17] is shown as the dashed histogram. The data points are the new H1 measurements [14].

which is *less steep* at NLO than LO. This is clear from figure 6 and tells us that there is a strong correlation between x-shapes of P_{qg} and g, implying that fixed order DGLAP for F_2 needs extreme flexibility of parton density parametrizations to offset the large NLO perturbative corrections at small x. The NLO steepness of P_{qg} is in fact the lowest order manifestation of NLO BFKL in the quark channel.

Recently progress has been reported in calculating the next-to-leading-log (NLL) contributions to the BFKL equation. Details may be found in [15]. Preliminary calculations seems to indicate that NLL contributions stem the leading order rise of the structure function ($x^{-\lambda}$ with $\lambda \simeq 0.5$) to $\lambda \simeq 2.65\alpha_s(Q)(1 - c\alpha_s(Q))$ with $c = 3.5$.

Thus detailed investigations into the phenomenological and conceptual issues regarding high energy log summations and more accurate signatures for BFKL evolution in the hadronic final state are needed. The selection criteria for these have to be such that they suppress the phase space for DGLAP evolution and maximize it for BFKL evolution.

One of these methods – the forward jet measurement has already been discussed. Preliminary results from H1 are shown in figure 7 and show a distinct preference for BFKL evolution, and is not reproduced by the DGLAP Monte Carlos.

The situation however is still far from clear. There are few theoretical calculations in resummed DGLAP. Most predictions for the final state observables are derived from Monte Carlo models whose drawback is their complexity and flexibility to model hadronization. This makes it difficult to pin down which feature of the theoretical input is being tested when compared with the data for the various Monte Carlos in the market like MEPJET,

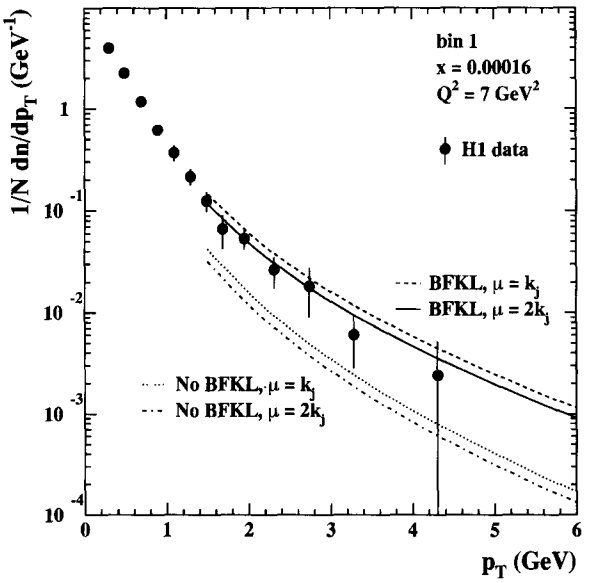

Figure 8. The transverse momentum spectrum of charged particles (π^+, π^-, K^+, K^-) in the pseudorapidity interval $0.5 < \eta < 1.5$ in the virtual photon–proton centre-of-mass frame – for details see [18].

HERWIG, LEPTO etc. On the other hand no Monte Carlo exist yet for BFKL evolution though some attempts have been made in that direction by ARIADNE. For a detailed discussion of forward jet events and its relevance to BFKL phenomenology, see [16].

5. Single particle spectrum at large p_T

Many of the ambiguities inherent in the forward jet event calculations mentioned above can be overcome by considering single particle emission at relatively large p_T in the central region. Such an event is more immune to hadronization effects and more directly reflects $\ln k_T^2$ diffusion from the BFKL ladder. The theoretical calculation has been done in [18] and preliminary data is shown in figure 8 for one value of x. There seems to be some evidence of $\ln(1/x)$ effects typical of BFKL evolution and diffusion. However it would be useful to compare this with the full fixed order calculation which would allow a clearer distinction between the different predictions. The full DGLAP calculation for this process has not yet been done and is presently under study [19].

6. Conclusion

In this talk we have concentrated on the various measurements of the structure funcions F_2 as also F_L. and compared them with various theoretical calculations corresponding to different evolution equations (DGLAP, BFKL..). The F_2 measurements alone, being 'too inclusive' are not sufficient to distinguish between different resummation programs, and 'less inclusive' events – in particular forward jet and single particle p_T spectrum as

signatures for distinguishing fixed order calculations like DGLAP with BFKL were discussed. They indicate that while there seems to be evidence of the $\ln 1/x$ type of evolution and k_T diffusion typical of BFKL, more theoretical calculations and more precise experimental results are needed before any conclusive evidence is obtained of the presence of BFKL effects.

Acknowledgement

The author would like to thank the organizers of WHEPP-5 for inviting him to the workshop and for providing an excellent atmosphere for work and interaction. A larger version of this talk is available at hep-ph/9805369.

References

[1] H1 Collaboration; T Ahmed *et al*, *Nucl. Phys.* **B429**, 477 (1994)
S Aid *et al*, *Nucl. Phys.* **B470**, 3 (1996)
[2] ZEUS Collaboration; M Derrick *et al*, *Phys. Lett.* **B315**, 481 (1993); *Z. Phys.* **C69**, 607 (1996)
[3] A Donnachie and P V Landshoff, *Nucl. Phys.* **B231**, 189 (1983); **B244**, 322 (1984); **B267**, 690 (1986); *Phys. Lett.* **B296**, 227 (1992); **B202**, 131 (1988)
[4] M Gluck, E Reya and A Vogt, *Z. Phys.* **C67**, 433 (1995)
[5] A D Martin, W J Stirling and R G Roberts, *Phys. Rev.* **D50**, 6734 (1994)
[6] Y L Dokshitzer, *Sov. Phys. JETP* **46**, 641 (1977)
[7] V N Gribov and L N Lipatov, *Sov. J. Nucl. Phys.* **15**, 438, 675 (1972)
G Altarelli and G Parisi, *Nucl. Phys.* **B126**, 298 (1977)
[8] V Fadin, E Kuraev and L Lipatov, *Sov. Phys. JETP* **44**, 443 (1976); **45**, 199 (1977)
Y Balitski and L Lipatov, *Sov. J. Nucl. Phys.* **28**, 822 (1978)
[9] A H Mueller, *Nucl. Phys.* **C18**, 125 (1990); *J. Phys.* **G17**, 1443 (1991)
[10] R D Ball and S Forte, *Phys. Lett.* **B335**, 77 (1994); *Phys. Lett.* **B336**, 77 (1994)
[11] A De Rujula *et al*, *Phys. Rev.* **D10**, 1649 (1974)
[12] Deep Inelastic Scattering at HERA, hep-ex/9712030
[13] A M Cooper-Sarkar, R C E Devenish and A De Roeck, *Structure Functions of the Nucleon and their Interpretation*, hep-ph/9712301
[14] H1 Collaboration; S Aid *et al*, *Phys. Lett.* **B356**, 118 (1995)
[15] There are a large number of papers on the NLL corrections to the BFKL LL result. An overview of these papers and the references can however be found in V. Del Duca, BFKL: a minireview, hep-ph/9706552
[16] V Del Duca, BFKL in forward jet production, hep-ph/9707348
[17] J Bartels *et al*, *Phys. Lett.* **B384**, 300 (1996) [hep-ph/9604272]
[18] J Kwiecinski, S C Lang and A D Martin, Single particle spectra in deep inelastic scattering as a probe of small x dynamics, hep-ph/9707240
[19] R Basu and R M Godbole, NLO-DGLAP calculation for single particle spectrum, in preparation